
Voxel-wise nonlinear analysis toolbox for neurodegenerative diseases and aging

Anonymous Author(s)

Affiliation

Address

email

Abstract

This paper describes a new neuroimaging analysis toolbox that allows for the modeling of nonlinear effects at the voxel level, overcoming limitations of methods based on linear models like the GLM. We illustrate its features using a relevant example in which distinct nonlinear trajectories of Alzheimer's disease related brain atrophy patterns were found across the full biological spectrum of the disease.

1 Introduction

Nowadays there is a vast armory of neuroimaging analysis tools available for the neuroscientific community whose ultimate goal is to conduct spatially extended statistical tests to identify regionally significant effects in the images without any a priori hypothesis on the location or extent of these effects. Some of these tools perform these tests at the voxel level¹, whereas some others provide with specific environments for analyzing the images, based on 3D meshes² or boundaries³.

Irrespective of these differences, the vast majority of neuroimaging tools are based on different implementations of the General Linear Model (GLM). Even though the GLM is flexible enough for conducting most of the typical statistical analysis, its flexibility for modeling nonlinear effects is rather limited. To this regard, it is important to note that some relevant confounders in most analysis, such as the impact of age on regional brain volumes, have been found to be better described by nonlinear processes [1, 2].

In this event, the most widely used alternative is to refrain from performing a voxel-wise analysis and quantify brain volumes based on regions of interest (ROIs) and then perform the nonlinear fitting of these trajectories by external software. This alternative has the obvious disadvantage that made voxel-wise analysis so popular on the first place: the need to identify a set of ROIs a priori.

In this work, we describe a new analysis toolbox that allows for the modeling of nonlinear effects at the voxel level that overcomes these limitations. In the following sections we briefly describe the main functionalities of the toolbox and illustrate its features using a relevant example in which distinct nonlinear trajectories are found as a function of a cerebrospinal fluid (CSF) related biomarker for participants in all stages of Alzheimer's disease (AD).

2 The toolbox

The toolbox comprises an independent fitting library, made up of different *model fitting* and *fit evaluation* methods, a processing module that interacts with the fitting library providing the formatted

¹<http://www.fil.ion.ucl.ac.uk/spm/>

²<http://freesurfer.net/>

³<http://idealab.ucdavis.edu/software/bbsi.php>

30 data obtained from the file system, several *visualization* tools and a command line interface that
31 allows the interaction between the user and the processing module, supported by a configuration file.

32 2.1 Model fitting techniques

33 Model fitting consists in finding a parametric or a nonparametric function of some explanatory
34 variables (predictors) and possibly some confound variables (correctors) that best fits the observations
35 of the target variable in terms of a given quality metric or, conversely, that minimizes the loss between
36 the prediction of the model and the actual observations. The models included in this toolbox are:

37 General Linear Model (GLM)

38 The General Linear model is a generalization of multiple linear regression to the case of more than
39 one dependent variable. Nonlinear relationships can be modeled within the GLM framework using a
40 polynomial basis expansion, mapping the input space into a feature space that includes the polynomial
41 terms of the variables.

42 Generalized Additive Model (GAM)

43 A Generalized Additive Model [3] is a Generalized Linear Model in which the observations of the
44 target variable depend linearly on unknown smooth functions of some predictor variables: $f(X) =$
45 $\alpha + \sum_{i=1}^k f_i(X_i)$. Here f_1, f_2, \dots, f_k are nonparametric smooth functions that are simultaneously
46 estimated using scatterplot smoothers by means of the backfitting algorithm [4]. Several fitting
47 methods can be accommodated in this framework by using different smoother operators, such as cubic
48 splines, polynomial or Gaussian smoothers.

49 Support Vector Regression (SVR)

50 In Support Vector Regression the goal is to find a function that has at most ϵ deviation from the
51 observations and, at the same time, is as flat as possible. However, the ϵ deviation constraint is not
52 feasible sometimes, and a hyperparameter C that controls the degree up to which deviations larger
53 than ϵ are tolerated is introduced. In the context of SVR nonlinearities are introduced with the "kernel
54 trick", that is, a kernel function $k(x_i, x_j) = \langle \Phi(x_i), \Phi(x_j) \rangle$ that implicitly maps the inputs from their
55 original space into a high-dimensional space. The kernel function used in this toolbox is the Radial
56 Basis Function (RBF) kernel, which is defined as $k(x_i, x_j) = \exp(-\gamma \|x_i - x_j\|^2)$.

57 SVR methods rely on several hyperparameters, namely ϵ and C in general and also γ when using a
58 RBF kernel function. To address the search of these hyperparameters an automatic method based
59 on grid search is included in this toolbox, which comprises the following steps: 1) sample the
60 hyperparameters space in a grid using one of the several sampling methods provided in the toolbox;
61 2) fit a subset of the data with the combination of hyperparameters of each sample in the grid; 3)
62 select the combination that minimizes the error function of choice. The lack of validation data and
63 the nature of morphometric data, which is vastly dominated by voxels with 0-valued observations,
64 limits the ability to find a subset of the data that is valid to find the optimal hyperparameters without
65 incurring in overfitting or underfitting. For that reason the following approach is taken: a subset of
66 m voxels is selected in each of the N iterations of the algorithm, the m selected voxels must contain
67 observations with a minimum variance of Var_{min} , and the error computed for each voxel is weighted
68 by the inverse of the variance of its observations.

69 2.2 Fit evaluation methods

70 The goodness of fit of a model can be evaluated using different metrics in order to create 3D statistical
71 maps, as shown in Figure 1.

72 MSE, Coefficient of determination (R^2)

73 These two metrics evaluate the predictive power of a model without penalizing its complexity.

74 Akaike Information Criterion (AIC)

75 The AIC is a criterion based on information theory widely used for model comparison and selection.
76 Unlike the previous metrics, it penalizes the complexity of the model by requiring its number of
77 parameters.

78 F-test

79 The F-test evaluates whether the variance of the full model (correctors and predictors) is significantly
80 lower — from a statistical point of view — than the variance of the restricted model (only correctors),
81 that is, the inclusion of the predictors contributes to the explanation of the observations. This statistical
82 test requires the degrees of freedom of both models, which are trivial to compute in GLM, but are not
83 in GAM or SVR. The equivalent degrees of freedom for Support Vector Regression are introduced in
84 the toolbox as defined in [5].

85 **Penalized Residual Sum of Squares (PRSS), Variance-Normalized PRSS**

86 Penalized Residuals Sum of Squares is introduced in the toolbox in order to provide a fit evaluation
87 metric that penalizes the complexity of the predicted curve without requiring the degrees of freedom.
88 However, PRSS is not suitable enough in the context of morphometric analysis, as it always provides
89 better scores for target variables with low-variance and flat trends than for target variables with
90 high-variance and nonflat trends, and that poses a problem as most of the voxels in the brain are
91 0-valued. For that reason a variance normalized version of the PRSS that weights the score with the
92 inverse of the variance of the predicted curve was introduced, the Variance Normalized Penalized
93 Residuals Sum of Squares.

94 **2.3 Model comparison and Interactive visualization tool**

95 The toolbox provides various methods to compare statistical maps generated using different fitting
96 models. These methods can be used, for instance, to select the best fitting model for each voxel,
97 to visualize the relative contribution of different models or to validate the similarity between two
98 statistical maps.

99 Moreover, an interactive visualization tool is included to give additional insight on the results: it
100 allows to load a 3D statistical map — generated with the fit evaluation method of choice or with a
101 comparison method — and one or several fitted models, and then plot the predicted curves of all the
102 models for the voxel selected with the cursor, hence easing the task of inspecting the curves in the
103 significant regions. An example of the aforementioned tool is found in Figure 2. Here, a best-fit map
104 is shown, where voxels are labeled according to the best fit score of three models under comparison
105 (polynomial GLM, polynomial SVR and Gaussian SVR). The bottom-right plot shows the trajectories
106 obtained for the three methods for the selected voxel and the corrected observations.

107 **3 Implementation details**

108 The whole toolbox has been implemented in Python. NumPy and SciPy libraries have been used for
109 the numerical and scientific computing, NiBabel to handle the morphometric data in NIfTI format,
110 scikit-learn ([6]) for the machine learning algorithms and matplotlib and seaborn for plotting and the
111 visualization features.

112 **4 A case study: atrophy patterns across the Alzheimer’s disease continuum**

113 To illustrate the toolbox functionalities, we analyze the nonlinear volumetric changes in gray matter
114 across the AD’s spectrum, following the approach proposed in [7]. Here, the subject’s level of
115 pathology and position along the AD continuum is represented by a CSF-related biomarker, the
116 AD-CSF index introduced in [8].

117 The dataset comprises 129 participants (62 controls, 18 preclinical AD, 28 mild cognitive impairment
118 (MCI) due to AD and 21 with diagnosed AD) who underwent MRI scanning and CSF analysis.
119 AD-CSF index was computed for all subjects applying the formula in [8], and the T1-weighted brain
120 scans of all participants were pre-processed using Voxel Based Morphometry (VBM) as implemented
121 in SPM8⁴. Further details of the dataset and the image processing pipeline can be found in [7].

122 Images of all the subjects were pooled together regardless of their diagnostic classification. We
123 first applied the same model proposed in [7], a polynomial GLM, entering age, sex, and the AD-CSF
124 index as regressors, modeling age as a second order polynomial to correct for the effects of aging on
125 gray matter content and the AD-CSF index as a third order polynomial. F-tests were used to analyze

⁴<http://www.fil.ion.ucl.ac.uk/spm>

the significant effects regarding the three AD-CSF index terms. Results were coherent with the ones found in [7].

In a second experiment we fitted a polynomial and a Gaussian SVR and computed their F-test statistical maps to compare their behaviour with the polynomial GLM. As an example, the map corresponding to the polynomial SVR is shown in Figure 1.

To compare the models, a best-fit map was obtained, assigning different numerical labels to voxels (label i is assigned if the best fit is for the i th model). Only voxels with a significance level lower than 0.001 located within clusters of more than 100 voxels are shown. An example of a voxel where the best score corresponds to the Gaussian SVR is presented in Figure 2, using the curve visualization tool.

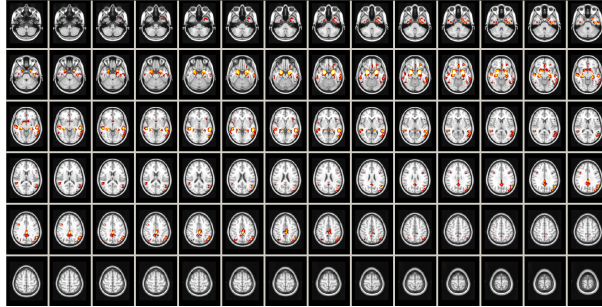


Figure 1: F-test statistical map for the polynomial SVR, with significance level (α) filtering at 0.001, minimum cluster size of 100 voxels and transformed into Z-scores for improved visualization.

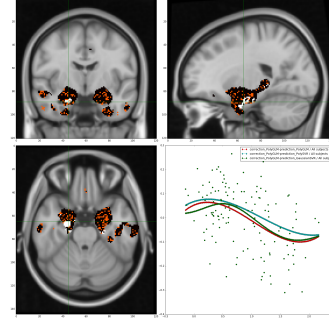


Figure 2: Comparison of polynomial GLM (black) vs polynomial SVR (orange) vs Gaussian SVR (white) with the corresponding curves for a voxel in which the best fitting score belongs to the Gaussian SVR model.

5 Conclusions

As compared to ROI-based statistical analysis, the voxelwise approach has the key advantage to allow for spatially unbiased analysis of brain images. This strategy has become predominant in the last decades and typically relies on particular implementations of the GLM. However, this approach presents limitations when it comes to the modeling of nonlinear effects, hence current neuroimaging analysis tools are sub-optimal for the identification of such nonlinear patterns. As a consequence, the capacity of neuroscientists to detect spatially distributed critical points associated to brain maturation or pathology is as well limited. In this context we understand that nonlinear modeling tools like the one that we are describing in this paper could be interesting and useful for the neuroimaging community.

As future work, we plan to extend the toolbox to deal with longitudinal data. The proliferation of neuroimaging repositories with longitudinal data provides with a unique opportunity for imaging researchers to analyze reference datasets with different tools, thus enabling the comparison and validation of analytical tools while gaining more insight on the data under analysis. Therefore, in the analysis of such longitudinal datasets, the availability of nonlinear modeling tools is likewise critical to fully understand the interrelationships between the trajectories of different biomarkers that may be crucial for understanding downstream pathological effects.

References

- [1] A. M. Fjell, L. T. Westlye, H. Grydeland, I. Amlie, T. Espeseth, I. Reinvang, N. Raz, D. Holland, A. M. Dale, and K. B. Walhovd. Critical ages in the life course of the adult brain: nonlinear subcortical aging. *Neurobiol. Aging*, 34(10):2239–2247, Oct 2013.
- [2] A. M. Fjell, L. T. Westlye, H. Grydeland, I. Amlie, T. Espeseth, I. Reinvang, N. Raz, A. M. Dale, and K. B. Walhovd. Accelerating cortical thinning: unique to dementia or universal in aging? *Cereb. Cortex*, 24(4):919–934, Apr 2014.
- [3] Trevor J Hastie and Robert J Tibshirani. *Generalized Additive Models*, volume 43 of *Monographs on Statistics and Applied Probability*. Chapman & Hall/CRC, June 1990.
- [4] L. Breiman and J.H. Friedman. Estimating optimal transformations for multiple regression and correlations (with discussion). *Journal of the American Statistical Association*, 80(391):580–619, 1985.
- [5] Francesco Dinuzzo, Marta Neve, Giuseppe De Nicolao, and Ugo Pietro Gianazza. On the representer theorem and equivalent degrees of freedom of svr. *Journal of Machine Learning Research*, 8:2467–2495, December 2007.
- [6] F. Pedregosa, G. Varoquaux, A. Gramfort, V. Michel, B. Thirion, O. Grisel, M. Blondel, P. Prettenhofer, R. Weiss, V. Dubourg, J. Vanderplas, A. Passos, D. Cournapeau, M. Brucher, M. Perrot, and E. Duchesnay. Scikit-learn: Machine learning in Python. *Journal of Machine Learning Research*, 12:2825–2830, 2011.
- [7] Juan Domingo Gispert, Lorena Rami, G Sánchez-Benavides, C Falcon, Alan Tucholka, S Rojas, and Jose L Molinuevo. Nonlinear cerebral atrophy patterns across the alzheimer’s disease continuum: impact of apoe4 genotype. *Neurobiology of Aging*, 36(10):2687–2701, October 2015.
- [8] Jose L Molinuevo, Juan Domingo Gispert, Bruno Dubois, Michael Heneka, Alberto Lleó, Sebastiaan Engelborghs, Jesús Pujol, Leonardo Cruz de Souza, Daniel Alcolea, Frank Jessen, Marie Sarazin, Foudil Lamari, Mircea Balasa, Anna Antonell, and Lorena Rami. The ad-csf-index discriminates alzheimer’s disease patients from healthy controls: a validation study. *Journal of Alzheimer’s Disease*, 36(1):67–77, June 2013.
- [9] Trevor Hastie, Robert Tibshirani, and Jerome Friedman. *The Elements of Statistical Learning. Data Mining, Inference, and Prediction*. Springer, second edition edition, February 2009.
- [10] Alex J. Smola and Bernhard Schölkopf. A tutorial on support vector regression. *Statistics and Computing*, 14(3):199–222, August 2004.